

Further studies of ATLAS Very Forward Detectors

Maciej Trzebiński

September 15, 2008

Contents

1	ATLAS Very Forward Detectors	3
1.1	Roman pots at 220 m	3
1.2	Absolute Luminosity for ATLAS	3
1.3	My tasks	3
2	Verification of results for standard LHC optics	4
2.1	Beam profiles	4
2.2	Protons behavior	4
2.3	Position in detector as a function of initial energy and position	9
2.3.1	Dependence on E	9
2.3.2	Dependence on x -slope	10
2.3.3	Dependence on x_0	11
3	Studies of the ALFA detector	14
3.1	Beam profiles	14
3.2	Protons behavior	14
3.3	Position in detector as a function of initial energy and position	18
3.3.1	Dependence on E	18
3.3.2	Dependence on x -slope	18
3.3.3	Dependence on x_0	20
4	Summary	22

1 ATLAS Very Forward Detectors

The ATLAS (A Toroidal LHC ApparatuS) experiment will measure collisions of two 7 TeV protons. The aim of the Very Forward Detectors (VFD) is to detect intact protons scattered at small angles. This will make possible to have some events with all particles in the final state measured.

Protons travel the distance between interaction point (IP) and detector in the beamline (in the magnetic field). The curvature of the proton that interacted will be different than the one that did not.

There are plans to install a few different VFD in the distance 200 – 500 m from the IP. The detectors are to be placed in the „Roman Pots” to be able to move the detectors close (about 1.5 mm) to the beam.

1.1 Roman pots at 220 m

This project contains four detectors (two on each side) located at 216 m and 224 m from the IP. Detectors will measure the horizontal (x) and vertical (y) position (z is the coordinate along the beamline) of protons at each plane with resolution of 10 μm .

1.2 Absolute Luminosity for ATLAS

Absolute Luminosity For ATLAS (ALFA) are the ATLAS ultra-small-angle detectors, which are to be located at 240 m on either side of the main ATLAS detector. They will measure elastically scattered protons for the primary purpose of absolute determination of the LHC luminosity at the ATLAS IP. „Roman Pots” inserts position sensitive detectors in the beam pipe. This will allow to detect scattered protons at small enough (mm) distances away from the circulating beam, to reach the theoretically well-calculable Coulomb scattering regime with the special LHC optics.

1.3 My tasks

The first task was to verify results produced by Rafał Staszewski during last year Sumer Student Program. I used a modified version of FPTrack (program for transport simulation written by Peter Bussey) code. FPTrack computes proton transport through the beamline using LHC optic files. I confirmed Rafał’s work using ”LHC Optic Version V6.500” for 7 TeV protons.

The next task was to perform the same analysis for ALFA. ALFA detector will be working with special high-beta optic. I investigated beam profiles, position dependence on E and p_T and I studied acceptance plots. Finally I found dependence of position in detector as a function of the initial energy, position and angle.

2 Verification of results for standard LHC optics

2.1 Beam profiles

Using beam characteristics at ATLAS IP for normal LHC run („LHC Optics Version V6.500 Collision” for 7 TeV protons) I generated a set of particle momenta that was used as an input to FPTrack. I used: $\sigma(x_0) = \sigma(y_0) = 16.6 \mu\text{ m}$, $\sigma(\Theta_x) = \sigma(\Theta_y) = 30.2 \mu\text{rad}$, $\sigma(E) = 0.77 \text{ GeV}$.

Magnets near ATLAS detector are shown in figure 1. The beam profiles can be seen in figure 2.

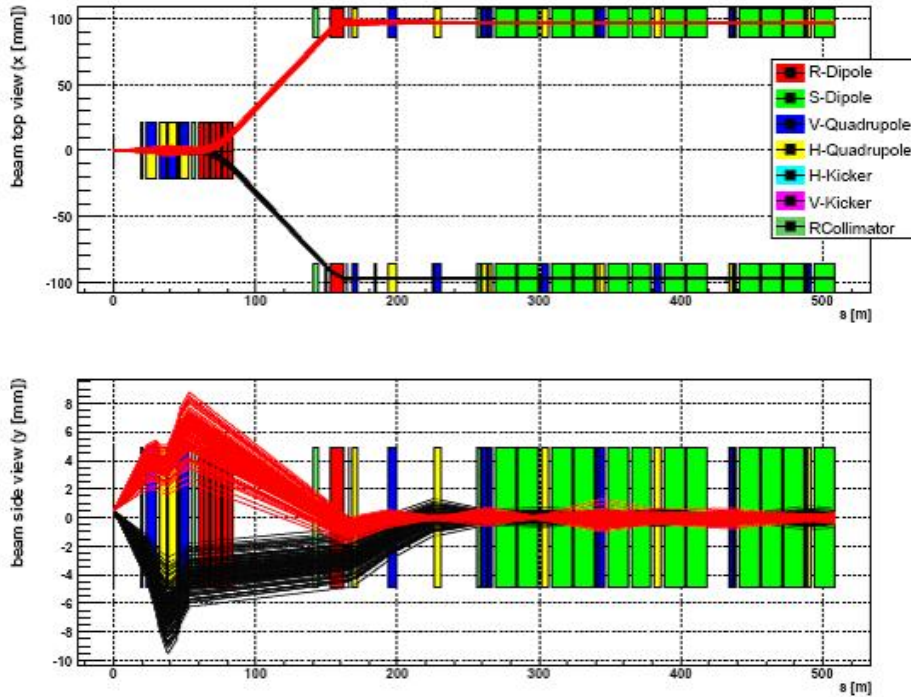


Figure 1: Magnets near ATLAS detector (red lines – beam no. 1, black lines – beam no. 2.).

2.2 Protons behavior

I studied protons position in the detectors plane as a function of their kinematics. I generated a set of momenta corresponding to $p_T = 0, 0.5, 1 \text{ GeV}$ and $E = 6.8, 6.9, 7 \text{ TeV}$. Results are presented in figure 3.

I also generated a set of momenta corresponding to p_T and E like above but with non-zero azimuthal angle $\phi \in [0; 2\pi)$ with step $2\pi/24$. Results are presented in figure 4.

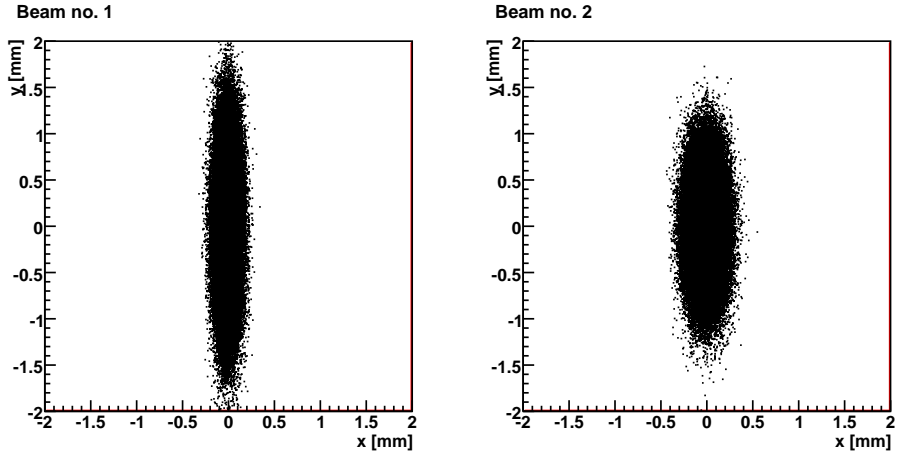


Figure 2: Beam profiles at 216 m.

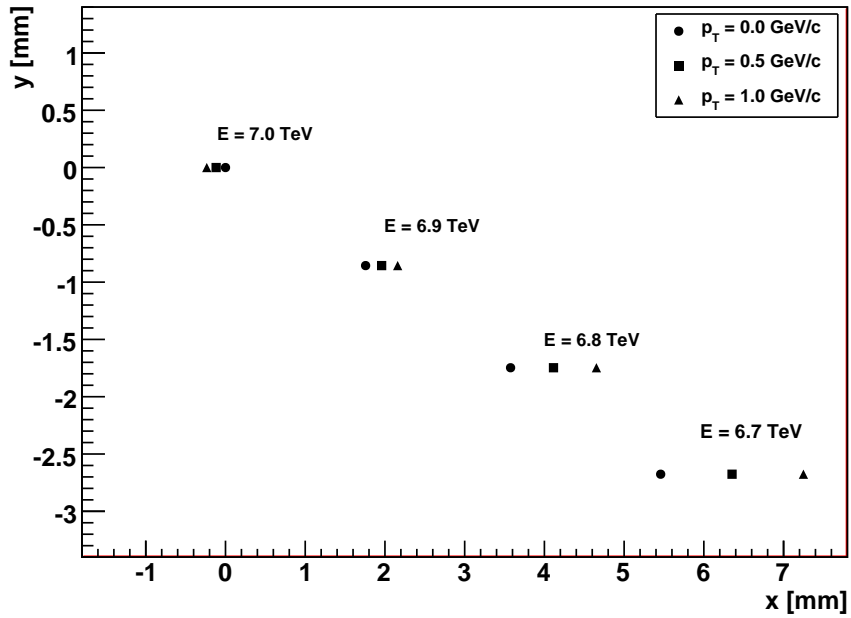


Figure 3: Position at 216 m for different p_T and E .

I was interested to find which protons can be seen at 216 m. In order to study this I created a plot of acceptance as a function of p_T and E . In this case acceptance is understood as a ratio of particles with given p_T and E observed on 216 m to the number of particles with the same p_T and E produced in the IP. The acceptance plot is shown in Figure 5. Since we cannot measure protons in main beam, I use cut for $|y| > 1.5$ mm (see Figure 6).

The other way for graphical transport parameterization are chromaticity plots. They are created by generating events with energy and angle (for chosen axis) taken from a Cartesian grid and transporting them to a chosen area. I generated a set of (E, x'_0) points for x (figure 7) and (E, y'_0) for y (figure 8). Lines with the same energy (angle) are connected giving chromaticity grid.

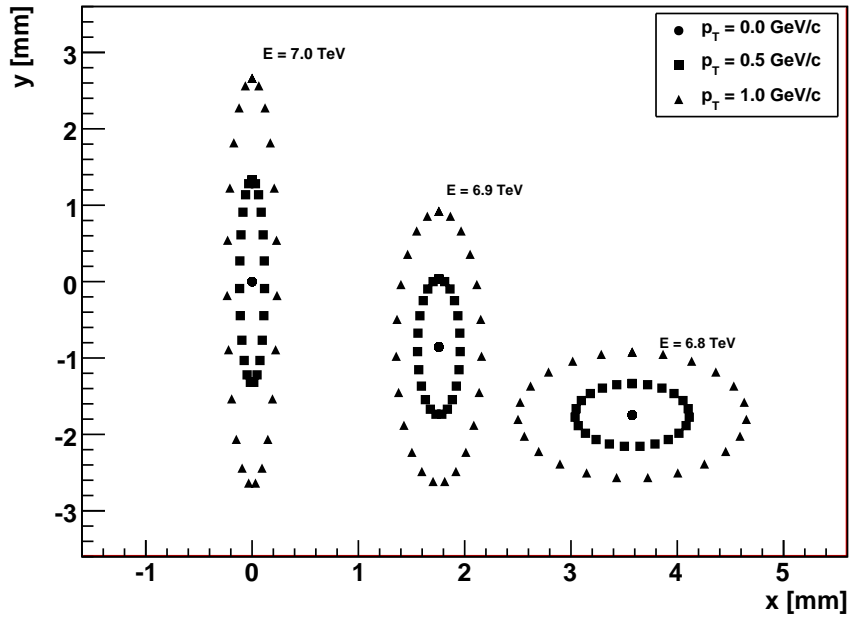


Figure 4: Position at 216 m for different p_T , E and $\phi \in [0; 2\pi)$.

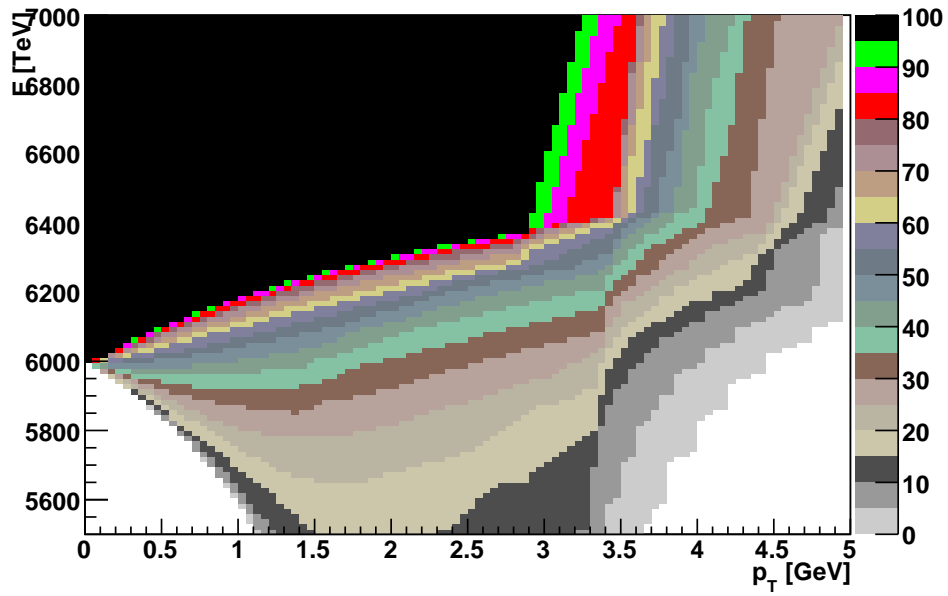


Figure 5: Acceptance at 216 m for beam no. 1.

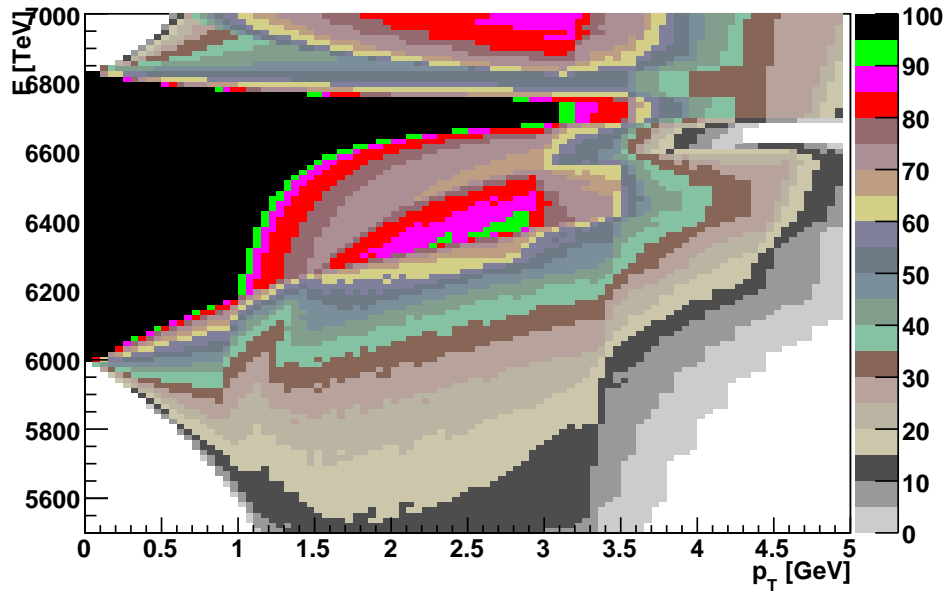


Figure 6: Acceptance at 216 m for beam no. 1 ($|y| > 1.5\text{mm}$).

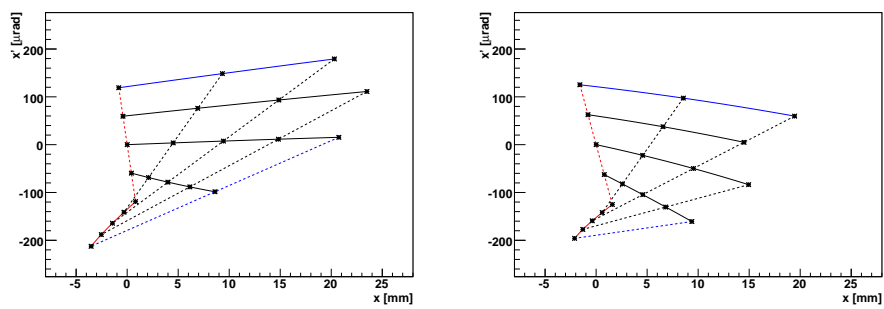


Figure 7: Chromaticity at 216 m for beam no. 1 (left) and no. 2 (right). Points of the same energy are connected with a solid line. Points of the same angle at the IP are connected with a dashed line.

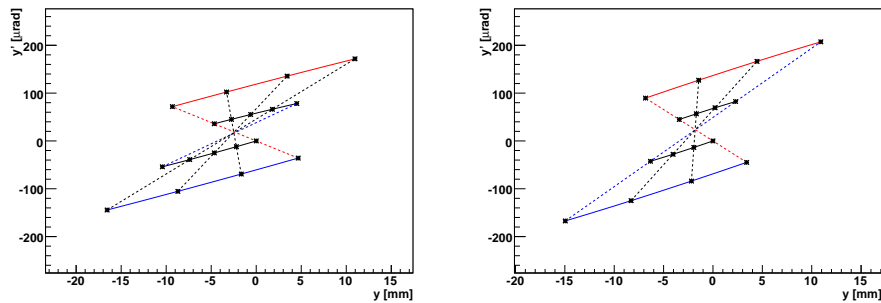


Figure 8: Chromaticity at 216 m for beam no. 1 (left) and no. 2 (right) Points of the same energy are connected with a solid line. Points of the same angle at the IP are connected with a dashed line.

2.3 Position in detector as a function of initial energy and position

Using FPTrack for computing positions of protons at the detector planes is time consuming. That is why I investigated the possibility of describing the position in the detector as a function of kinematics at the IP.

$$x'_0 = \frac{p_x}{p_z} \quad (1)$$

$$x_0 - \text{position of the IP} \quad (2)$$

2.3.1 Dependence on E

I checked the dependence of the x -position on E (for $x'_0 = 0$ and $x_0 = 0$). The results are shown in figure 9 where I also present a fitted cubic polynomial defined in equation 3. The figure on the right shows the difference between FPTrack and fit values. The degree of the polynomial is the smallest one that gave errors below $10\mu\text{m}$ (which is the detector resolution). Values of the coefficients of the fitted polynomial can be found in table 1.

$$x(E) = a_0 + a_1E + a_2E^2 + a_3E^3 \quad (3)$$

Coefficient	Value
a_0	$4.835268 \cdot 10^2$
a_1	$-1.531573 \cdot 10^{-1}$
a_2	$1.662796 \cdot 10^{-5}$
a_3	$-6.594669 \cdot 10^{-10}$

Table 1: $x(E)$ fit coefficients.

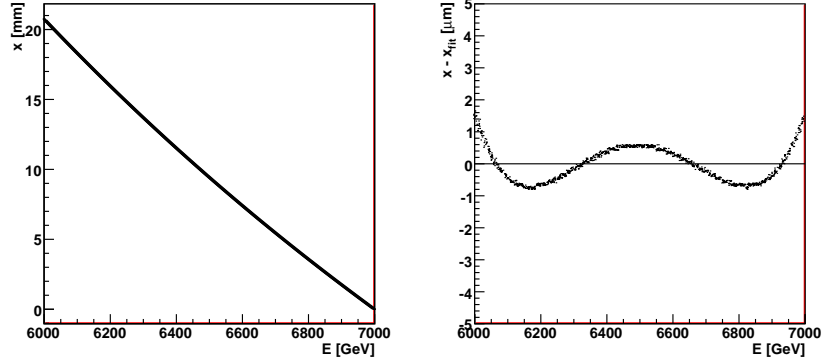


Figure 9: Dependence of x on E .

2.3.2 Dependence on x -slope

I checked how x position depends on the x'_0 for different E (figure 10). The linear fit was good enough to fit the data (see figure 11) with sufficiently small error.

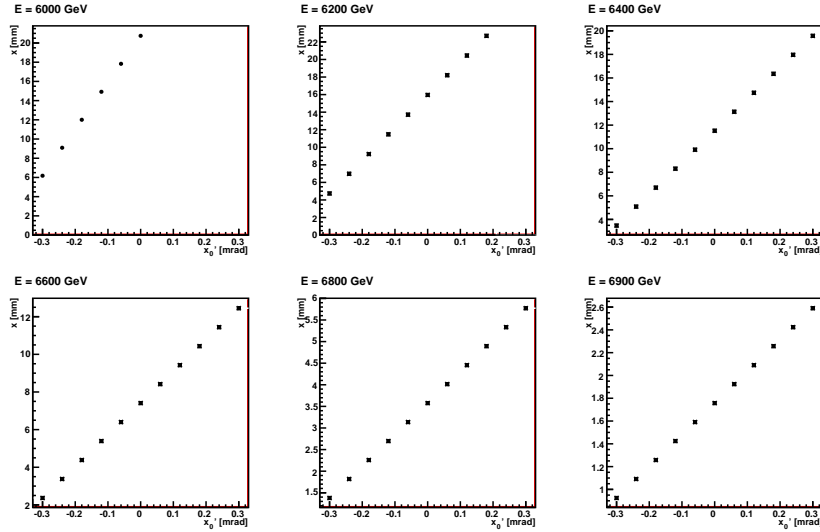


Figure 10: Dependence of x on x'_0 for few different energies.

The next step was to find how coefficients change with changing energy:

$$x(x'_0, E) = x(E) + B(E)x'_0 \quad (4)$$

For each plot I compute linear regression slope coefficient. In figure 12 I present this coefficients as a function of E . I fitted the distribution with a cubic polynomial:

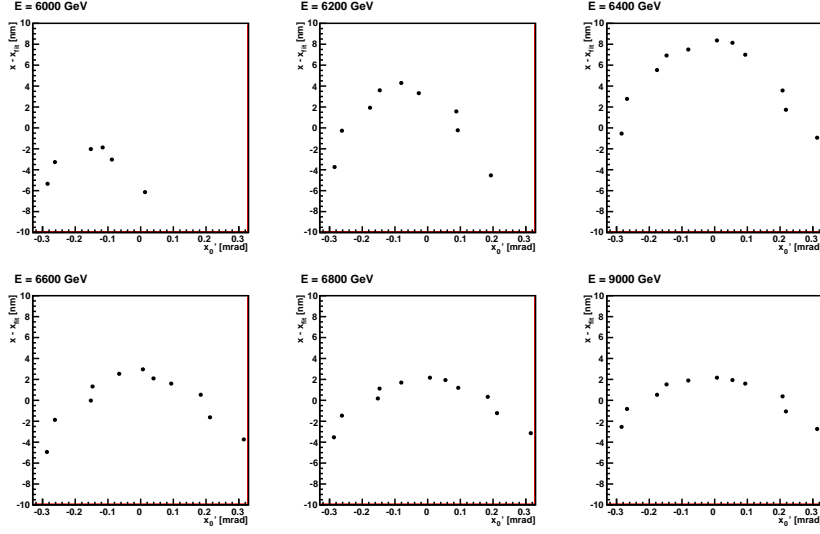


Figure 11: Dependence of x on x'_0 – fit error.

$$B(E) = B_0 + B_1E + B_2E^2 + B_3E^3 \quad (5)$$

Values of the coefficients can be found in table 2.

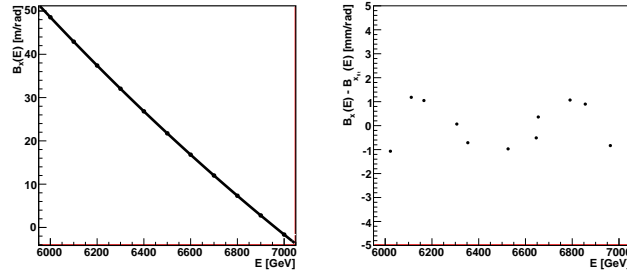


Figure 12: Dependence of x on x'_0 for different energies.

2.3.3 Dependence on x_0

Finally I investigated the dependence on x_0 . The linear fit was good enough to fit the data (see figure 13).

$$x(x_0, E) = x(E) + C(E)x_0 \quad (6)$$

In figure 14 I present these coefficients as a function of E . I fitted the distribution with a cubic polynomial:

Coefficient	Value
b_0	$7.425955 \cdot 10^2$
b_1	$-1.879737 \cdot 10^{-1}$
b_2	$1.436254 \cdot 10^{-5}$
b_3	$-3.853871 \cdot 10^{-10}$

Table 2: $B(E)$ fit coefficients.

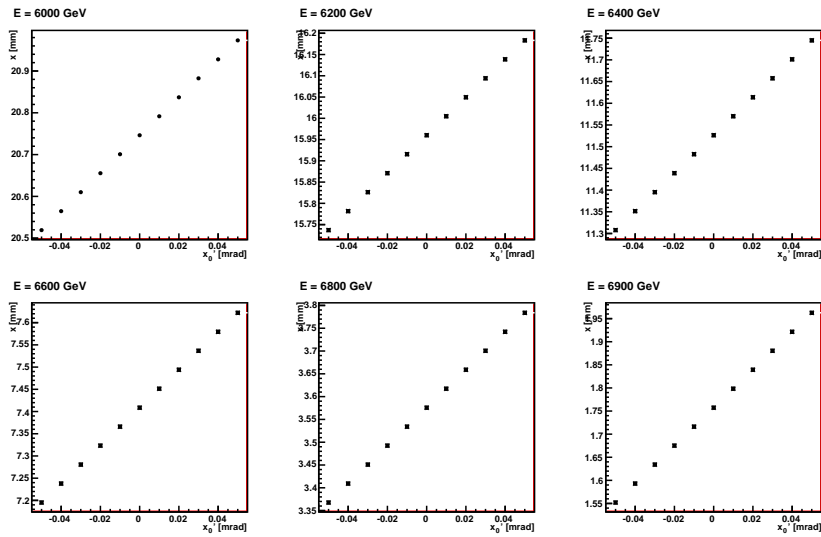


Figure 13: Dependence of x on x_0 for few different energies.

$$C(E) = C_0 + C_1 E + C_2 E^2 + C_3 E^3 \quad (7)$$

Values of the coefficients can be found in table 3.

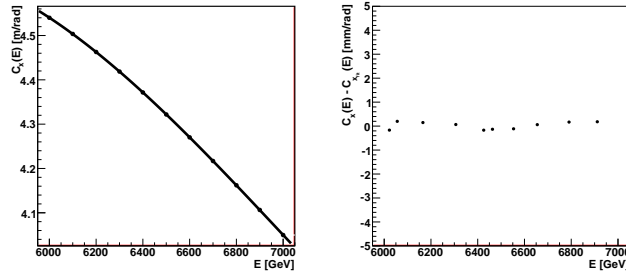


Figure 14: Dependence of x on x'_0 for different energies.

Coefficient	Value
c_0	$-1.574817 \cdot 10^{-6}$
c_1	$9.577077 \cdot 10^{-9}$
c_2	$-1.443628 \cdot 10^{-13}$
c_3	$6.850247 \cdot 10^{-17}$

Table 3: $C(E)$ fit coefficients.

3 Studies of the ALFA detector

3.1 Beam profiles

Using beam characteristics at ATLAS IP for high-beta LHC run I generated a set of particle momenta that was used as an input to FPTrack. I used: $\sigma(x_0) = \sigma(y_0) = 0.061$ mm, $\sigma(\Theta_x) = \sigma(\Theta_y) = 0.23$ μ rad, $\sigma(E) = 0.77$ GeV.

The beam profiles can be seen in figure 15.

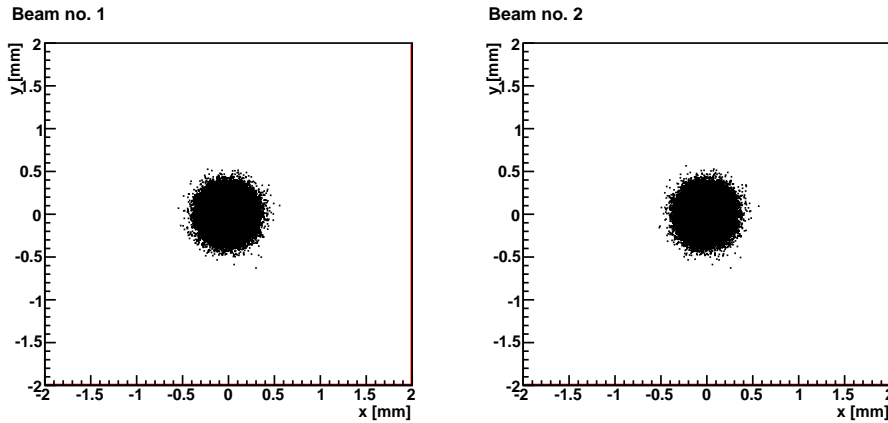


Figure 15: Beam profiles at 240 m.

3.2 Protons behavior

I studied protons position in the detectors plane as a function of their kinematics. I generated a set of momenta corresponding to $p_T = 0, 0.025, 0.05$ GeV and $E = 6.7, 6.8, 6.9, 7$ TeV. Results are presented in figure 16.

I also generated a set of momenta corresponding to p_T and E like above but with different azimuthal angle $\phi \in [0; 2\pi)$ with step $2\pi/24$. Results are presented in figure 17.

I was interested to find which protons can be seen at 240 m. In order to study this I created a plot of acceptance as a function of p_T and E . In this case acceptance is understood as a probability of observing particles with given p_T and E at 240 m. The acceptance plot is shown in figure 18. Since we cannot measure protons in main beam, I use cut for $|y| > 1.5$ mm (see figure 19).

I also generated physical events using PYTHIA MC generator. I selected non-dissociative protons from a single diffraction process (proc. 93). Acceptance plots are in figure 20 and figure 21.

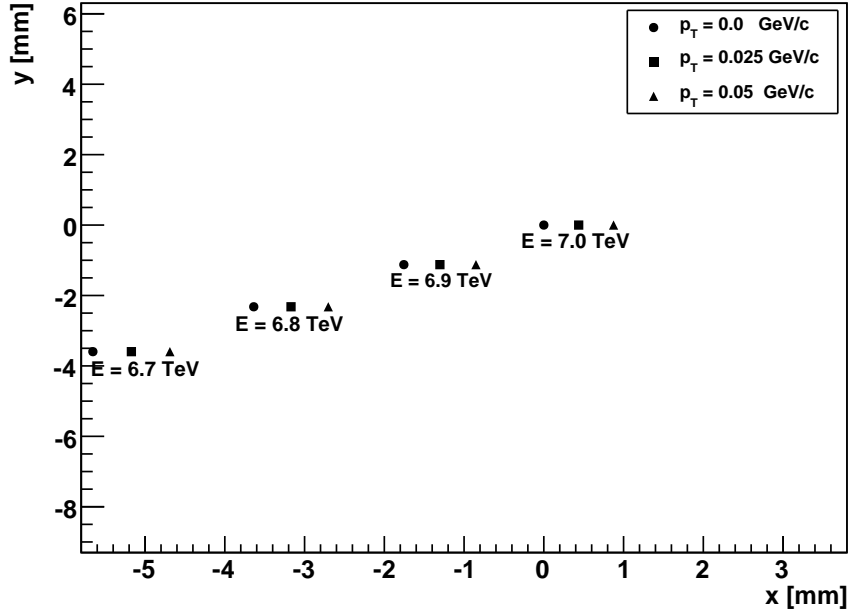


Figure 16: Position at 240 m for different p_T and E .

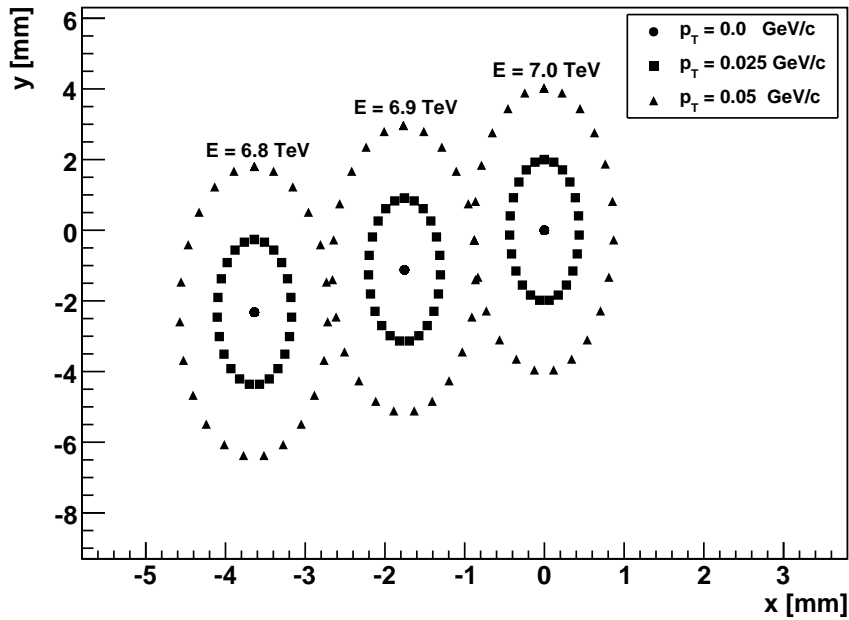


Figure 17: Position at 240 m for different p_T and E for $\phi \in [0; 2\pi)$.

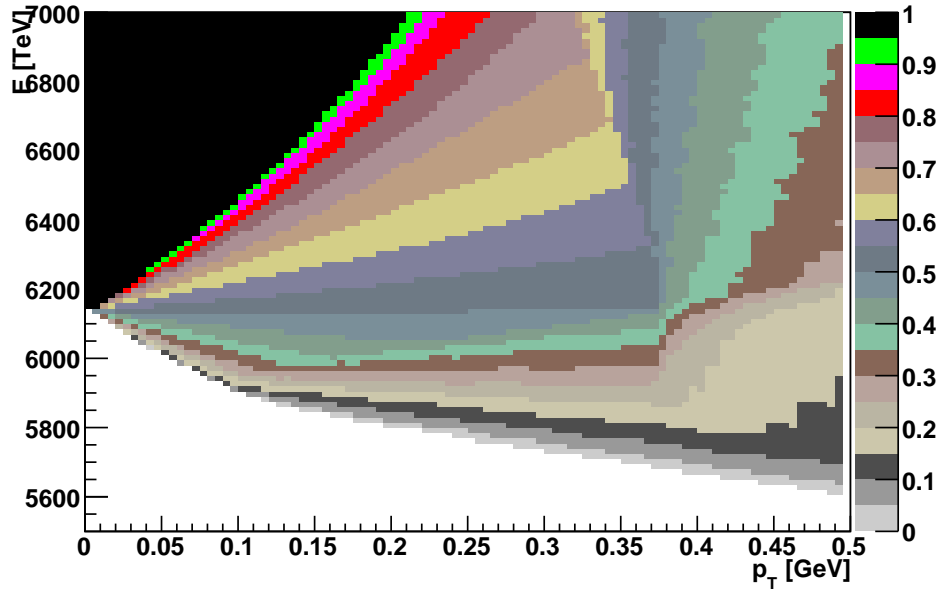


Figure 18: Acceptance at 240 m for beam no. 1.

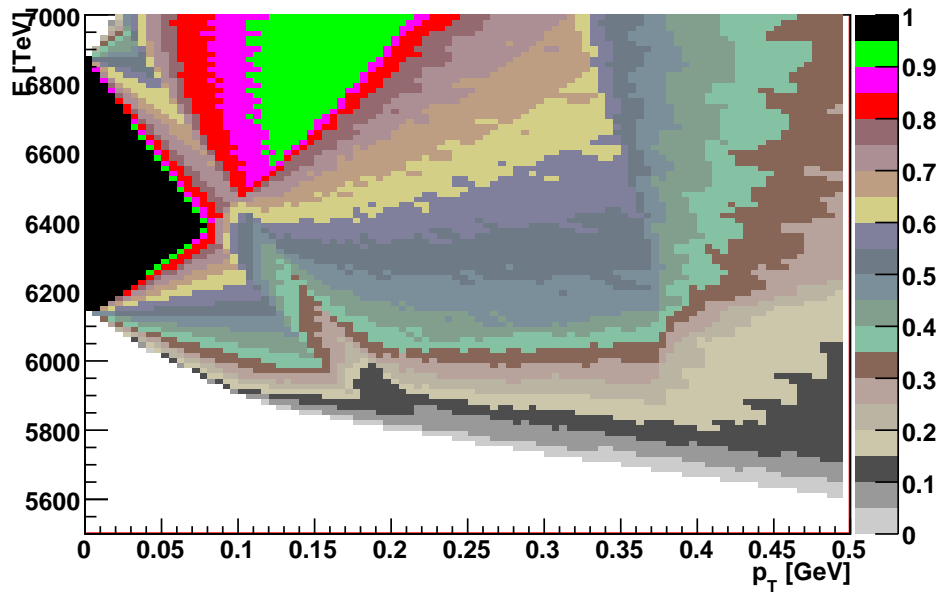


Figure 19: Acceptance at 240 m for beam no. 1 ($|y| > 1.5mm$).

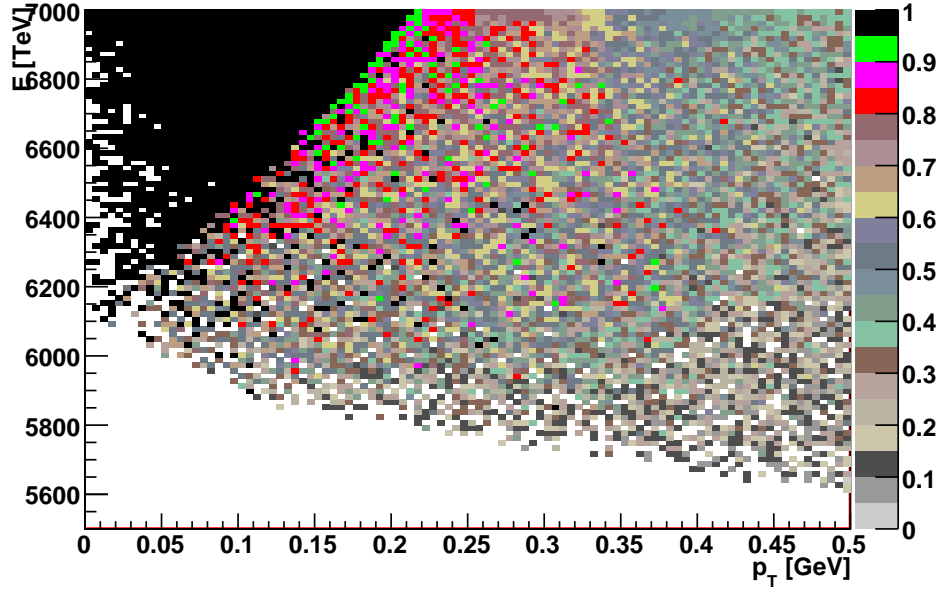


Figure 20: Acceptance at 240 m for beam no. 1 (PYTHIA MC).

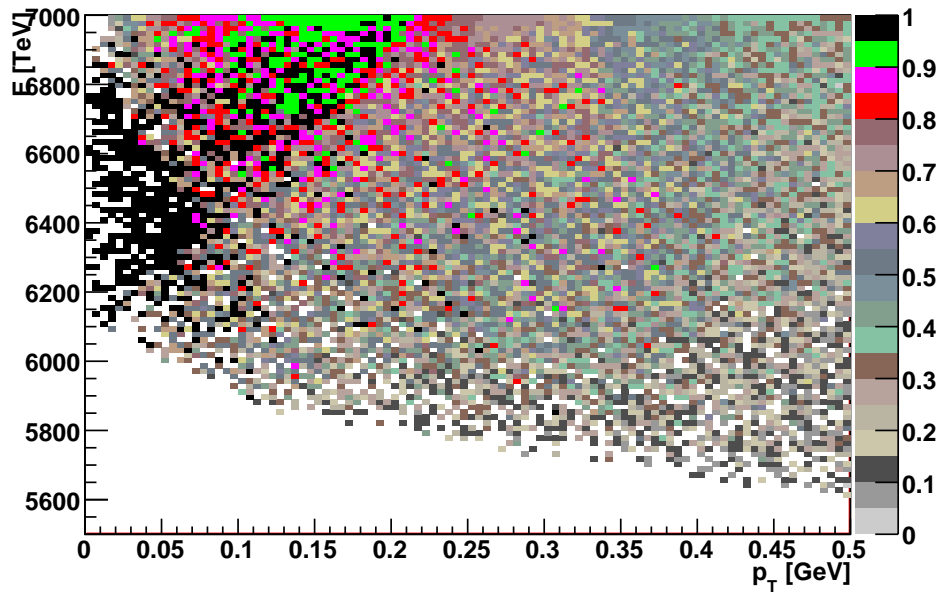


Figure 21: Acceptance at 240 m for beam no. 1 ($|y| > 1.5mm$) (PYTHIA MC).

3.3 Position in detector as a function of initial energy and position

I investigated the possibility of describing the position in the detector as a function of kinematics at the IP.

3.3.1 Dependence on E

I checked the dependence on the x -position on E (for $x'_0 = 0$ and $x_0 = 0$). The results are shown in figure 22 where I also present a fitted cubic polynomial defined in equation 3. The figure on the right shows the difference between FPTrack and fit values. The degree of the polynomial is the smallest one that gave errors below $10\mu m$ (which is the detector resolution). Values of the coefficients of the fitted polynomial can be found in Table 4.

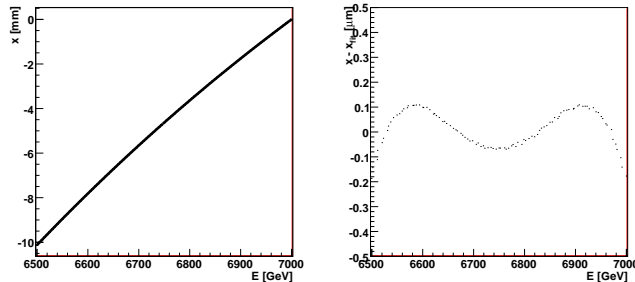


Figure 22: Dependence on x on E .

Coefficient	Value
a_0	$-8.956236 \cdot 10^2$
a_1	$3.086196 \cdot 10^{-1}$
a_2	$-3.576431 \cdot 10^{-5}$
a_3	$1.421976 \cdot 10^{-9}$

Table 4: $x(E)$ fit coefficients.

3.3.2 Dependence on x -slope

I checked how x position depends on the x'_0 for different E (Figure 23). The linear fit was good enough to fit the data (see Figure 24) with a sufficiently small error.

The next step was to find how coefficients change with changing energy:

For each plot I computed linear regression slope coefficient. In figure 25 I present this coefficients as a function of E . I fitted the distribution with a cubic polynomial 5.

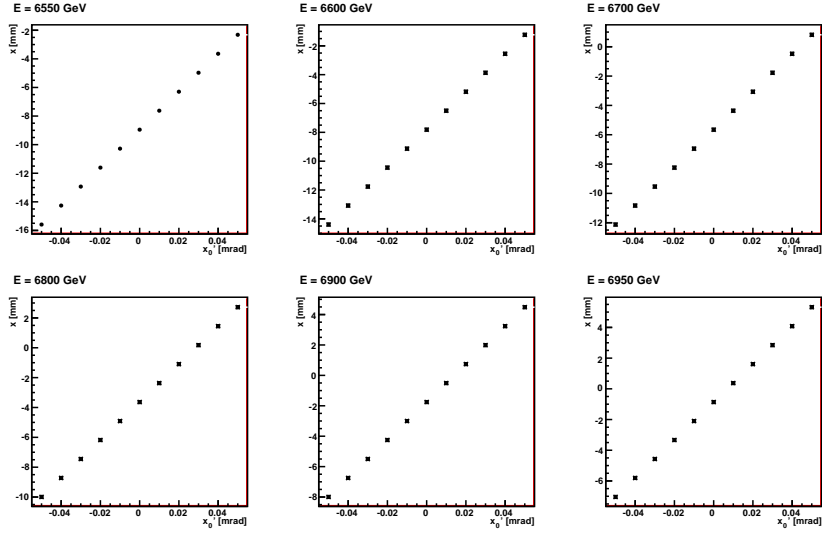


Figure 23: Dependence on x on x'_0 for few different energies.

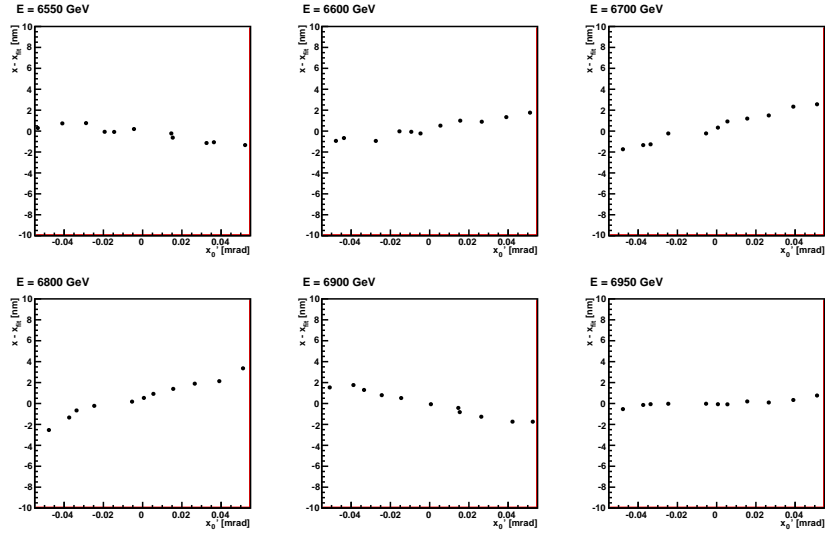


Figure 24: Dependence on $x - x_{fit}$ on $x'_0 - \text{fit error}$.

Values of the coefficients can be found in table 5 and fit error in figure 25.

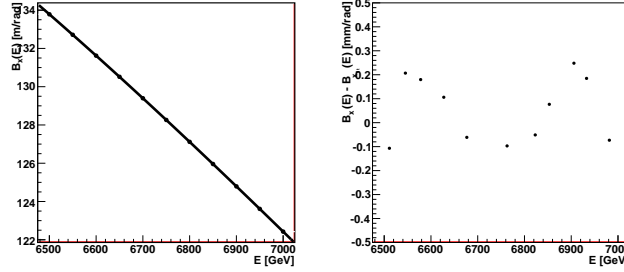


Figure 25: Dependence on $B_x(E)$ on E and fit error.

Coefficient	Value
b_0	$-2.288562 \cdot 10^2$
b_1	$1.873498 \cdot 10^{-1}$
b_2	$-2.861954 \cdot 10^{-5}$
b_3	$1.289187 \cdot 10^{-9}$

Table 5: $B(E)$ fit coefficients.

3.3.3 Dependence on x_0

Finally I investigated the dependence on x_0 . The linear fit was good enough to fit the data (see figure 26 and 27).

For each plot I computed linear regression slope coefficient. In figure I present these coefficients as a function of E . I fitted the distribution with a quadratic polynomial:

$$C(E) = C_0 + C_1E + C_2E^2 \quad (8)$$

Values of the coefficients can be found in table 6.

Coefficient	Value
c_0	-8.979846
c_1	$2.312172 \cdot 10^{-3}$
c_2	$-1.432485 \cdot 10^{-7}$

Table 6: $C(E)$ fit coefficients.

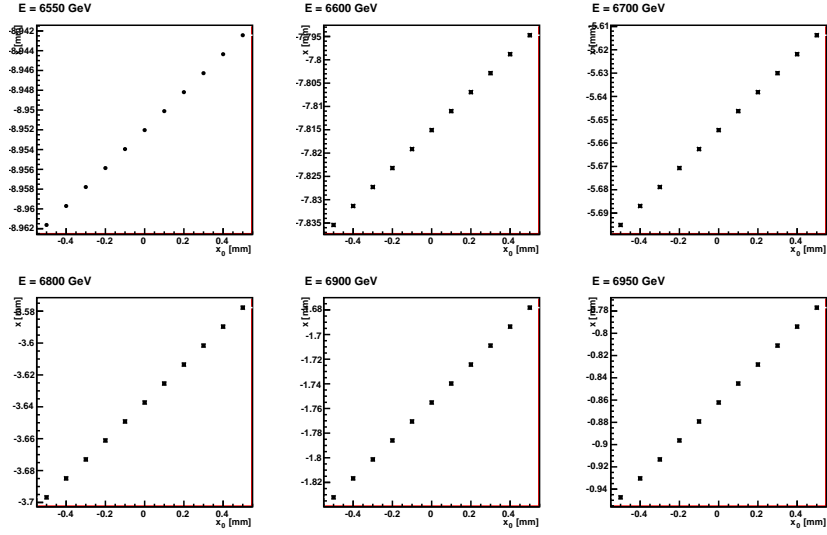


Figure 26: Dependence on x on x_0 for few different energies.

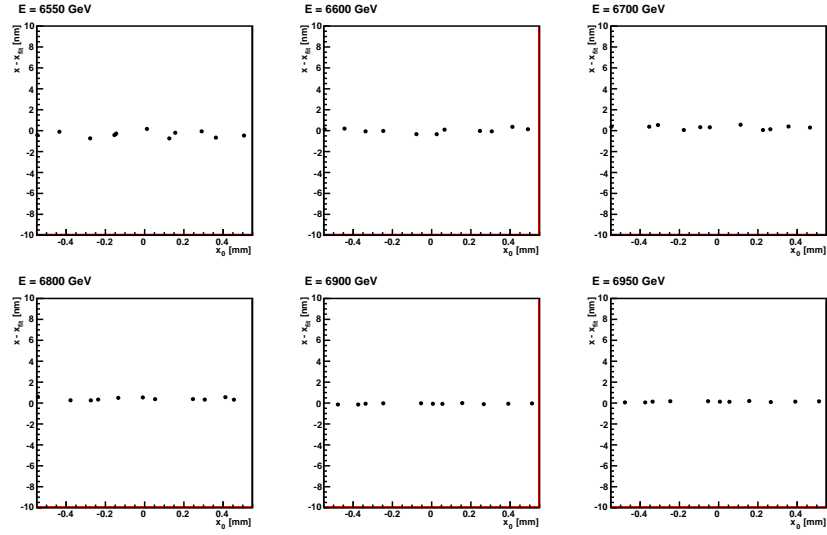


Figure 27: Dependence on $x - x_{fit}$ on $x_0 - \text{fit error}$.

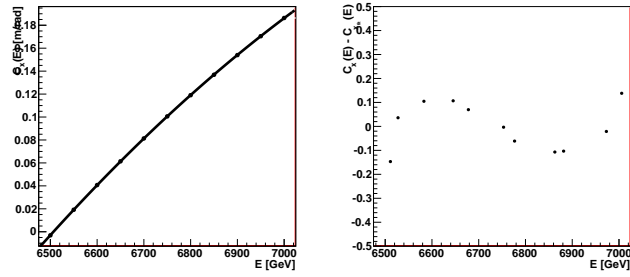


Figure 28: Dependence on $C_x(E)$ on E and fit error.

4 Summary

Beam profiles, acceptance and position reconstruction in the ATLAS forward detectors were studied.